



Verification of NWP Model Analyses and Radiosonde Humidity Data with GPS Precipitable Water Vapor Estimates during AMMA

Olivier Bock, M. Nuret

► To cite this version:

Olivier Bock, M. Nuret. Verification of NWP Model Analyses and Radiosonde Humidity Data with GPS Precipitable Water Vapor Estimates during AMMA. *Weather and Forecasting*, 2009, 24 (4), pp.1085-1101. 10.1175/2009WAF2222239.1 . hal-03973874

HAL Id: hal-03973874

<https://hal.science/hal-03973874>

Submitted on 5 Feb 2023

HAL is a multi-disciplinary open access archive for the deposit and dissemination of scientific research documents, whether they are published or not. The documents may come from teaching and research institutions in France or abroad, or from public or private research centers.

L'archive ouverte pluridisciplinaire **HAL**, est destinée au dépôt et à la diffusion de documents scientifiques de niveau recherche, publiés ou non, émanant des établissements d'enseignement et de recherche français ou étrangers, des laboratoires publics ou privés.



Verification of NWP Model Analyses and Radiosonde Humidity Data with GPS Precipitable Water Vapor Estimates during AMMA

O. BOCK

LAREG, IGN, Marne-la-Vallée, France

M. NURET

CNRM, Météo-France, Toulouse, France

(Manuscript received 4 December 2008, in final form 18 March 2009)

ABSTRACT

This paper assesses the performance of the European Centre for Medium-Range Weather Forecasts-Integrated Forecast System (ECMWF-IFS) operational analysis and NCEP-NCAR reanalyses I and II over West Africa, using precipitable water vapor (PWV) retrievals from a network of ground-based GPS receivers operated during the African Monsoon Multidisciplinary Analysis (AMMA). The model analyses show reasonable agreement with GPS PWV from 5-daily to monthly means. Errors increase at shorter time scales, indicating that these global NWP models have difficulty in handling the diurnal cycle and moist processes at the synoptic scale. The ECMWF-IFS analysis shows better agreement with GPS PWV than do the NCEP-NCAR reanalyses (the RMS error is smaller by a factor of 2). The model changes in ECMWF-IFS were not clearly reflected in the PWV error over the period of study (2005–08). Radiosonde humidity biases are diagnosed compared to GPS PWV. The impacts of these biases are evidenced in all three model analyses at the level of the diurnal cycle. The results point to a dry bias in the ECMWF analysis in 2006 when Vaisala RS80-A soundings were assimilated, and a diurnally varying bias when Vaisala RS92 or Modem M2K2 soundings were assimilated: dry during day and wet during night. The overall bias is offset to wetter values in NCEP-NCAR reanalysis II, but the diurnal variation of the bias is observed too. Radiosonde bias correction is necessary to reduce NWP model analysis humidity biases and improve precipitation forecast skill. The study points to a wet bias in the Vaisala RS92 data at nighttime and suggests that caution be used when establishing a bias correction scheme.

1. Introduction

Numerical weather prediction (NWP) models play an increasing role in our everyday life. Short- to medium-range weather forecasts are used to anticipate severe weather events, which have increasing socioeconomic impacts within the context of climate change and variability. NWP models serve also as the basis for developing seasonal weather prediction and climate projection systems, which both are of crucial importance for vulnerable regions, such as the Sahel. NWP model analyses are also extensively used for scientific research, either as large-scale forcings for mesoscale atmospheric simulations in case study experiments or as a full three-dimensional

description of the atmospheric and surface parameters for climate research. In this latter case, reanalyses are of special interest since they are produced with a fixed version of an NWP model and the only changes in analysis and forecast performance result from changes in the observations that are assimilated. Within the framework of the African Monsoon Multidisciplinary Analyses (AMMA; information online at <http://www.amma-international.org>), NWP models thus play a crucial role in many scientific research areas.

One of the main objectives of AMMA is that of improving our knowledge of land, ocean, and atmosphere processes and the interactions of the West African monsoon (WAM) system (Redelsperger et al. 2006). The skill of NWP models in predicting rainfall over West Africa, and the tropics in general, is especially low. One of the main reasons is that the major part of precipitation is convective and that the forecast models

Corresponding author address: Olivier Bock, LAREG, IGN, 6-8 Ave. Blaise Pascal, Marne la Vallée 77455, France.
E-mail: olivier.bock@ign.fr

have difficulty in handling the development of convection, especially over land, where it is badly phased with the diurnal cycle (Yang and Slingo 2001). Over West Africa, NWP models generally locate the intertropical convergence zone (ITCZ) too far to the south. This is observed both in NWP analyses and forecasts, though the forecasts from both ECMWF model and the Action de Recherche Petite Echelle–Grande Echelle (ARPEGE) model of Météo-France have a tendency to migrate the ITCZ to the north (but not enough compared to the observations) during the first few forecast days (Tompkins et al. 2005; Nuret et al. 2007; Agusti-Panareda and Beljaars 2008). Errors in the analyses are partly due to systematic errors in observations [e.g., radiosonde biases; Bock et al. (2007)] or to deficiencies in the assimilation systems [e.g., radiative transfer calculations for satellite radiances; Andersson et al. (2005)]. Another limiting factor, especially over West Africa, is the lack of observations for properly constraining the vertical thermodynamic and wind structures in the analyses. In this respect, radiosonde data are of prime importance. This motivated AMMA scientists to upgrade and reactivate the West African radiosonde network for the AMMA enhanced and special observing periods (EOPs and SOPs, respectively). Hence, 21 stations were active during the SOP, from June to September 2006, from which ~7000 soundings were made (Parker et al. 2008). During this period, seven stations made four soundings per day, and six of them increased their frequency to eight soundings per day during two intensive periods (20–29 June and 1–15 August 2006). The other stations usually made one or two soundings per day. Improvements in telecommunication systems allowed a substantial increase in the number of soundings transmitted through the Global Telecommunication Service (GTS) to NWP centers for assimilation since March 2006 (and throughout 2007). In addition to the enhanced radiosoundings, many other observations were made during AMMA, among which some also entered into the operational NWP models. As a consequence, there is much interest in using NWP model analyses and forecasts during AMMA since their performance is expected to be improved compared to past periods.

In the present paper we focus on atmospheric humidity, which is one essential component of the West African monsoon (WAM) water cycle, and assess its representation in three largely used NWP models: the European Centre for Medium-Range Weather Forecasts–Integrated Forecast System (ECMWF–IFS), the National Centers for Environmental Prediction–National Center for Atmospheric Research (NCEP–NCAR) reanalysis I [referred to as NCEP1; Kalnay et al. (1996)], and the NCEP–Department of Energy (DOE) reanalysis II [referred to

as NCEP2; Kanamitsu et al. (2002)]. To this end, we use special observations collected during the AMMA EOP. However, the assessment of NWP models makes sense only when independent observations are used. Hence, in the present work we use precipitable water vapor (PWV) estimates provided by a network of ground-based global positioning system (GPS) receivers, the data of which are not presently assimilated into the currently used NWP models. The GPS technique is known to provide very accurate estimates of PWV (usually considered at the level 1–2 kg m⁻²) with high temporal resolution (typically hourly) and all-weather capability (Klein Baltink et al. 2002; Haase et al. 2003; Hagemann et al. 2003; Deblonde et al. 2005; Bock et al. 2007; Macpherson et al. 2008). However, GPS PWV estimates do not give insight into the vertical distribution of humidity. To assess the vertical distribution of humidity in the NWP models, it may therefore be necessary to use radiosonde data at sites where GPS receivers were operated. Radiosonde humidity data are known to exhibit dry and wet biases, depending on the type and age of the sondes, and on the environmental conditions of use (Wang et al. 2002). Since radiosonde data are assimilated into NWP models, their biases can be transferred to the NWP model analyses and can impact subsequent forecasts (Andersson et al. 2005, 2007; Bock et al. 2007). Both dry and wet biases have been evidenced in the AMMA radiosonde network operated during summer 2006 using the GPS PWV estimates (Bock et al. 2008a). In the present work we extend the verification of radiosonde PWV estimates throughout the EOP and investigate their impacts on all three model analyses.

The present work complements the previous studies in the following aspects. In Bock et al. (2007), we assessed various observational and NWP reanalysis datasets [namely, 40-yr ECMWF Re-Analysis (ERA-40) and NCEP2] using GPS data from the International Global Navigation Satellite Systems Service (IGS; information online at <http://igsceb.jpl.nasa.gov/>) network (i.e., sparsely distributed over Africa). In the present work, we extend the verification of radiosonde data and NWP model analyses over West Africa thanks to the AMMA GPS stations during the more recent years (with the exception that ERA-40 was stopped in 2002 and we thus used the ECMWF operational analysis). In Bock et al. (2008a), we assessed mainly the ARPEGE operational analysis from Météo-France during the 2006 monsoon season.

The organization of the paper is as follows. Section 2 introduces the datasets and the methodology used for the intercomparison. Section 3 compares NWP model analyses to observations. Section 4 investigates the impact of radiosonde biases on NWP model analyses.

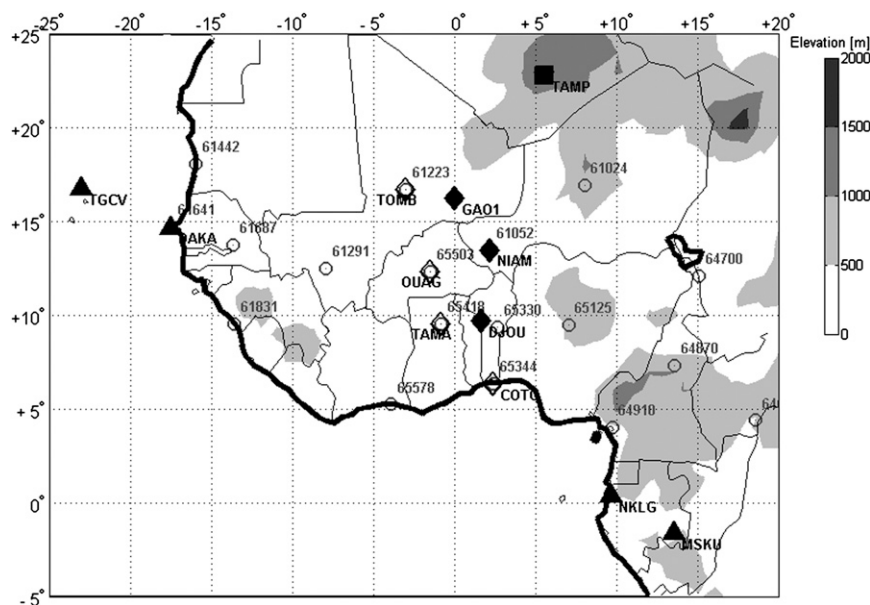


FIG. 1. Map showing the locations of GPS receivers and radiosonde stations in operation during the AMMA EOP (2005–07). The GPS sites are indicated as symbols with four-letter identifiers (IDs) and the radiosonde sites are indicated as circles with five-digit IDs. The GPS sites comprise four IGS sites (filled triangles), three AMMA-EOP sites (filled diamonds), three AMMA-SOP sites (open diamonds), TAMP (square), an Algerian permanent station, and COTO (open diamond), an AMMA test station installed in 2005. Gray shading shows topography (see axis on the right).

Section 5 concludes and discusses the main results from this work and outlines subsequent work on the radiosonde biases correction and further NWP model assimilation experiments.

2. Data and analysis method

The locations of the GPS stations used in this study are shown in Fig. 1. Six of these GPS receivers have been established over West Africa within the framework of AMMA (Bock et al. 2008a). Among the other stations, DAKA is a permanent station whose data are available through the IGS, and TAMP is a permanent station operated by the Centre de Recherche en Astronomie, Astrophysique et Géophysique, Algeria (CRAAG), whose data have been made available through the French Institut National des Sciences de l'Univers (INSU). The AMMA GPS receivers have been deployed along the meridian climatic gradient between the Guinean coast and the Sahara in order to monitor the total atmospheric humidity in different climatic areas and investigate atmospheric processes at a broad range of time scales, from subdiurnal to seasonal. The characteristics of the GPS systems and details of the related data processing are given in Bock et al. (2008a). For the present work, we use the most

accurate GPS solution [referred to as reprocessed in Bock et al. (2008a)], which comprises the AMMA GPS stations as well as DAKA and TAMP. The conversion of the GPS zenith tropospheric delay (ZTD) estimates into PWV quantities is done using the mean tropospheric temperature, T_m , estimated from ECWMF operational analyses provided by the Technical University of Vienna (information online at <http://mars.hg.tuwien.ac.at/~ecmwf1/>) and surface pressure observed at the location of the AMMA GPS receivers (these measurements are provided by a dedicated weather station attached to the GPS station). At DAKA and TAMP, surface pressure observations were either not available or not trustable and thus surface pressure from ECWMF operational analysis is used instead. The accuracy of the surface variables from the different NWP models is assessed in section 3 below. The accuracy of the GPS PWV estimates used here is believed to be at a level of $\pm 0.5 \text{ kg m}^{-2}$ on average along with a random component that might reach $\pm 1 \text{ kg m}^{-2}$ on a single estimate [based on intercomparison with other observational data; see references quoted above, and the assessment of the GPS data processing discussed in Bock et al. (2008a)]. Note that the use of ECMWF analyses in the conversion from ZTD into PWV introduces a correlation in GPS PWV estimates to errors

in this model analyses. However, as discussed in Bock et al. (2008a), this procedure is much more accurate than using a simplistic linear function of the surface temperature for T_m (Bevis et al. 1994). For example, a rather large error of 3 K (1%) in T_m might produce a maximum error of 0.5 kg m^{-2} (1% of 50 kg m^{-2}).

For the present work we also used high-resolution radiosonde data retrieved by the Agence pour la Sécurité de la Navigation Aérienne en Afrique et à Madagascar (ASECNA) in collaboration with national weather services since 2006. These sites are also represented in Fig. 1. The high-resolution (2 s) data files contain up to 3000 levels (roughly 100 times more than the TEMP messages transmitted from the stations through the GTS to the NWP centers). We thinned the profiles down to 50-m vertical resolution up to 7-km altitude and 100 m above, leading to ~ 220 levels from the surface up to 18 km. For the comparison with GPS PWV, we integrated the radiosonde water vapor density observations from the height of the GPS station up to 18 km. We followed the methodology described in Bock et al. (2007), for the interpolation near the surface and detection of outliers in the radiosonde (RS) data. The high-resolution radiosonde files contain additional information such as the serial numbers of the sondes, which can be decoded into the type and age of the sonde. We used this kind of information to stratify among sonde types. A further refinement using sonde age was not made here, mainly because for some sonde types the number of sondes per class would have been too small. Note that the radiosonde data used in this work are not corrected for known biases or ground calibration errors. The comparison to GPS PWV is thus representative of the quality of the high-resolution radiosonde data as assimilated in operations and also presently available in the AMMA database.

The NWP models used in this study are well known and will not be described extensively. For the ECMWF-IFS we refer the reader to the ECMWF Web site (<http://www.ecmwf.int/research/ifsdocs/>), and for the NCEP-NCAR reanalyses we refer the reader to Kalnay et al. (1996) and Kanamitsu et al. (2002), for versions I and II of the reanalyses, respectively. The main differences that we may highlight between these assimilation systems and forecast models are the following. The ECMWF-IFS is based on a four-dimensional variational data assimilation system (4DVAR), which determines the model trajectory that minimizes the differences in the observations in a 12-h time window. The model had 60 vertical levels from the surface up to 10 Pa and a spectral truncation of T511 (i.e., horizontal resolution of $\sim 35 \text{ km}$) before 1 February 2006. Since that date, the model has been improved to include 91 vertical levels

from the surface up to 10 Pa and a spectral truncation of T799 (i.e., horizontal resolution of $\sim 25 \text{ km}$). The model is upgraded several times a year (9 times between 1 January 2005 and 31 December 2008), with the aim of continuously improving the performance of both the assimilation and forecasting systems (details and the expected impacts of changes may be found online: http://www.ecmwf.int/products/data/technical/model_id/index.html). A major change, in view of the present work, is the introduction of a radiosonde humidity correction on 6 November 2007 (cycle 32r3), along with an important modification to the convection scheme for the tropics (Bechtold et al. 2008). The principles of this and other correction schemes are discussed at the end the paper. More details on the ECMWF bias correction scheme and its validation are described in Agusti-Panareda et al. (2009).

Compared to ECMWF-IFS, the NWP model used for the production of the NCEP-NCAR reanalyses might appear as of an older generation. However, the fact that the assimilation and forecast system remain unchanged has a substantial advantage over operational systems, in that the performance of the model is nearly constant over time. The changes may be attributed to changes only in the observing system. Hence, reanalyses are best suited for climate studies and the investigation of interannual variability (Higgins et al. 1996; Trenberth and Guillemot 1998; Roads et al. 2002). The NCEP-NCAR reanalyses use a 3DVAR system with 28 vertical levels from the surface up to 3 Pa and a spectral truncation of T62 (i.e., horizontal resolution of $\sim 210 \text{ km}$). Because it has coarser horizontal resolution, fewer surface stations are assimilated in regions of steep topography. There are many differences also in the parameterizations and the treatment of surface variables over land (e.g., the way soil moisture is adjusted from the observations). For what concerns the water cycle, NCEP2 is usually considered to be superior to NCEP1, with namely higher PWV contents over the tropics (Kanamitsu et al. 2002).

For the present work, we used ECMWF-IFS analysis extracted on various regular latitude-longitude grids. The NCEP-NCAR reanalyses were only available at $2.5^\circ \times 2.5^\circ$. For the intercomparison of model-analyzed PWV fields with GPS PWV, a common $2.5^\circ \times 2.5^\circ$ grid is thus used; the impact of horizontal resolution is discussed separately based on ECMWF data. The horizontal and vertical displacements between GPS stations and the nearest model grid points are reported in Table 1. The four grid points surrounding the GPS station are actually used. A correction ΔPWV is calculated at each grid point, which accounts for the difference in the surface elevation between the grid points and the GPS

TABLE 1. Location and coordinates of the GPS stations, and horizontal and vertical displacements (model – GPS) to the nearest model grid points (both models are used on a similar $2.5^\circ \times 2.5^\circ$ grid). The stations are ordered by increasing latitude.

Location	GPS				Model – GPS displacement		
	ID	Lat ($^\circ$ N)	Lon ($^\circ$ E)	Alt (m MSL)	Distance (km)	Δh (ECMWF) (m)	Δh (NCEP) (m)
Tamale, Ghana	TAMA	9.6	–0.9	170	107	0	–89
Djougou, Benin	DJOU	9.7	1.7	436	98	90	139
Ouagadougou, Burkina Faso	OUAG	12.4	–1.5	305	108	27	–33
Niamey, Niger	NIAM	13.5	2.2	223	114	–8	–28
Dakar, Senegal	DAKA	14.7	–17.5	16	35	15	–28
Gao, Mali	GAO1	16.3	0.0	260	139	–143	–118
Timbuktu, Mali	TOMB	16.7	–3.0	264	101	14	–24
Tamanrasset, Algeria	TAMP	22.8	5.5	1381	63	367	488

station. The four corrected PWV values are then interpolated horizontally to the latitude and longitude of the GPS station using a bilinear interpolation method. The correction Δ PWV is calculated following the methodology presented in Bock et al. (2007). It is scaled to the difference in elevation, Δh ; the surface humidity, ρ_v ; and PWV. This vertical correction is able to correct for significant (up to $2\text{--}3 \text{ kg m}^{-2}$) differences between NWP model fields and GPS observations over Africa (Bock et al. 2007). The horizontal interpolation introduced here further corrects systematic differences of $0.5\text{--}1 \text{ kg m}^{-2}$ in magnitude and reduces consistently the NWP model biases diagnosed with respect to GPS PWV. The temperature, humidity, and surface pressure are interpolated in a similar way.

3. Assessment of NWP models

a. Surface meteorological parameters

Before assessing the PWV fields from the three NWP models, we first verify the 2-m temperature (T) and relative humidity (RH), which enter into the correction for vertical displacement between the model topography and GPS station height. Table 2 shows the average differences of all three NWP model analyses (at $2.5^\circ \times 2.5^\circ$ resolution) and observations collected by GPS weather stations. Overall, one can see that the RH and T from the ECMWF model analysis are in excellent agreement with the observations at all stations. The RH bias is about $\pm 2\%$ and the standard deviation of the differences is smaller than 10%. The bias and standard deviation of the differences in T reach 0.8 and 2.1 K, respectively. The correlation coefficient is quite high ($r \geq 0.88$) if we consider that this comparison includes the diurnal cycle, which is usually poorly represented in such models. This good agreement is not very surprising knowing that surface observations [from surface synoptic observation (SYNOP) stations] are assimilated

into the ECMWF-IFS and that these data have a significant weight. Very few other observations (except radiosonde data and some satellite radiances) actually have an impact on near-surface parameters, especially humidity (Andersson et al. 2007). However, the present comparison is meaningful in the sense that the data from surface sensors used here did not go into the models (we did not use observations from the SYNOP stations). Moreover, the calibration of these sensors was properly controlled during AMMA. Interestingly, one may notice that the standard deviation of the RH and T differences increases as one moves from the south to the north of the domain. This fact might reveal increased difficulty in the model's ability to handle these atmospheric parameters in the Sahel, especially at the time scale of the diurnal cycle. This difficulty is probably linked to both the scarcity of the SYNOP observing network and problems in physical parameterizations during the rainy season (note that the comparison is performed during June–September). Surface pressure from the ECMWF-IFS analysis was also evaluated (not shown) and resulted in similar fair agreement with the observations (the standard deviation of the differences was smaller than 0.7 hPa but biases of up to 2.5 hPa were observed at some sites).

The comparison for the NCEP–NCAR reanalyses reveals slightly larger discrepancies in both RH and T . NCEP2 performs slightly better than NCEP1 and, in particular, shows an increasing standard deviation of differences with latitude, similar to ECMWF-IFS. Among the reasons for the larger discrepancy is the coarser horizontal resolution in the native numerical model (2.5° for NCEP–NCAR reanalyses compared to $\sim 0.25^\circ$ for ECMWF-IFS), inducing increased differences in the representativeness between the model fields and point observations, and the differences in the model physics and data assimilation systems. The latter differences might also partly explain the differences between the two NCEP–NCAR reanalyses.

TABLE 2. The 2-m RH (%) and temperature ($^{\circ}\text{C}$) differences between NWP model analyses (at horizontal resolution of $2.5^{\circ} \times 2.5^{\circ}$) and the observations (from dedicated weather stations near the six AMMA GPS stations). The computations are made for 6-hourly data from June to September 2005–07. The mean difference (BIAS), computed as model – observation; std dev; and correlation (r) are given. The total number of data pairs is similar for all three models (ranging between 489 and 1129, depending on station). The stations are ordered by increasing latitude.

Station	ECMWF						NCEP1						NCEP2					
	RH			T			RH			T			RH			T		
	BIAS	Std dev	r	BIAS	Std dev	r	BIAS	STD	r	BIAS	Std dev	r	BIAS	Std dev	r	BIAS	Std dev	r
TAMA	0.4	6.2	0.88	0.8	1.5	0.88	8.5	10.8	0.61	−0.3	2.1	0.74	6.3	9.7	0.68	−0.1	2.2	0.70
DJOU	1.1	6.3	0.89	0.2	1.4	0.90	4.6	13.1	0.34	−0.8	2.5	0.65	6.9	10.5	0.63	−0.9	2.4	0.71
OUAG	1.4	8.1	0.89	−0.1	1.7	0.91	10.5	14.6	0.71	−1.1	2.6	0.79	6.3	12.0	0.76	−0.3	2.7	0.74
NIAM	−1.0	8.5	0.90	0.2	1.9	0.91	7.7	11.5	0.81	−1.1	2.4	0.83	5.3	12.1	0.76	−0.5	2.7	0.78
GAO1	−2.2	9.2	0.90	0.3	2.1	0.90	−1.0	11.2	0.84	0.2	2.5	0.86	1.3	11.9	0.82	0.1	2.5	0.85
TOMB	−1.3	9.7	0.90	0.0	1.8	0.94	−1.8	12.4	0.83	0.3	2.5	0.87	−0.8	15.8	0.71	−0.4	3.2	0.77

The uncertainty in surface RH and T from the NWP models will translate into additional error in the PWV correction term, ΔPWV , accounting for the height difference Δh with the GPS antenna. This error can be assessed using the empirical relationship $\Delta\text{PWV}/\text{PWV} = -40\%$ per 1000 m (see Bock et al. 2007). Assuming an uncertainty of 10% in the correction term due to errors in RH and T , a height difference of $\Delta h = 100$ m and a total $\text{PWV} = 50 \text{ kg m}^{-2}$ would result in an error in ΔPWV of 0.2 kg m^{-2} . Considering the differences in elevation of the nearest model grid points (Table 1), one can estimate that the root-mean-square error (RMSE) associated with the correction for vertical displacement is smaller than 0.5 kg m^{-2} for all three models, including differences in representativeness.

b. Precipitable water vapor

The time evolution of PWV estimated from GPS stations GAO1, NIAM, and DJOU, and corresponding values from the NWP model analyses (ECMWF, NCEP1, and NCEP2), are shown in Fig. 2, from 2005 to 2008. The data have been smoothed over a 5-day period, in order to highlight the gross features in the seasonal cycle and intraseasonal variability. Figure 2 also includes the precipitation rate from the Global Precipitation Climatology Project [GPCP; Huffman et al. (1997); available until April 2008 only]. One can recognize in Fig. 2 the main features of the WAM, both in terms of atmospheric humidity and precipitation, which are tightly correlated parameters. As highlighted in Bock et al. (2008a), PWV is a defining measure of the monsoon system dynamics from which five distinct phases can be determined in the wet season cycle. The moist air mass associated with the monsoon onset usually arrives in April in the region of Djougou, Benin, and in May in the region of Niamey, Niger, and Gao, Mali. It is followed by a relatively stationary period until the air mass

progresses again toward the north of the continent around the end of June and beginning of July. This period coincides with the onset of the rainy season over the Sahel (12° – 20°N) as defined by Sultan and Janicot (2003). It is followed by the core of the rainy season over the Sahel (July to mid-September) during which 10–20-day modulations in PWV and precipitation are evident during all 4 yr (except for 2008, when no GPCP data are available). The last monsoon phase is the retreat of the moist air mass and, consequently, the end of rainfall. A full discussion of the interannual variability and intra-seasonal modulations seen in Fig. 2 is beyond the scope of this paper. However, we must mention that the seasonal cycles and, most notably, the dry to wet season transition periods are significantly different in terms of PWV variations between these 4 yr, with 2005 and 2006 being especially different from 2007 and 2008.

Figure 2 shows that all three models reproduce quite well the gross features of the seasonal cycle, especially the wet season. Significant differences in PWV are observed during the dry season between the two NCEP–NCAR reanalyses and GPS, whereas the ECMWF operational analysis follows very closely the time variations and magnitude of the PWV observed with the GPS. The better agreement of the ECMWF model analysis with GPS observations might be linked to differences in forecast models and assimilation systems and, possibly, also to differences in the types of data assimilated. The much finer horizontal resolution of the native ECMWF model (T511 before 1 February 2006 and T799 after) might allow the assimilation of much more data in the ECMWF operational analysis (especially from SYNOP stations and radiosondes in the boundary layer), since a major reason for black-listing surface data is linked to the differences in elevation between the sensor and the model's orography. Differences in the quantity and quality of the data

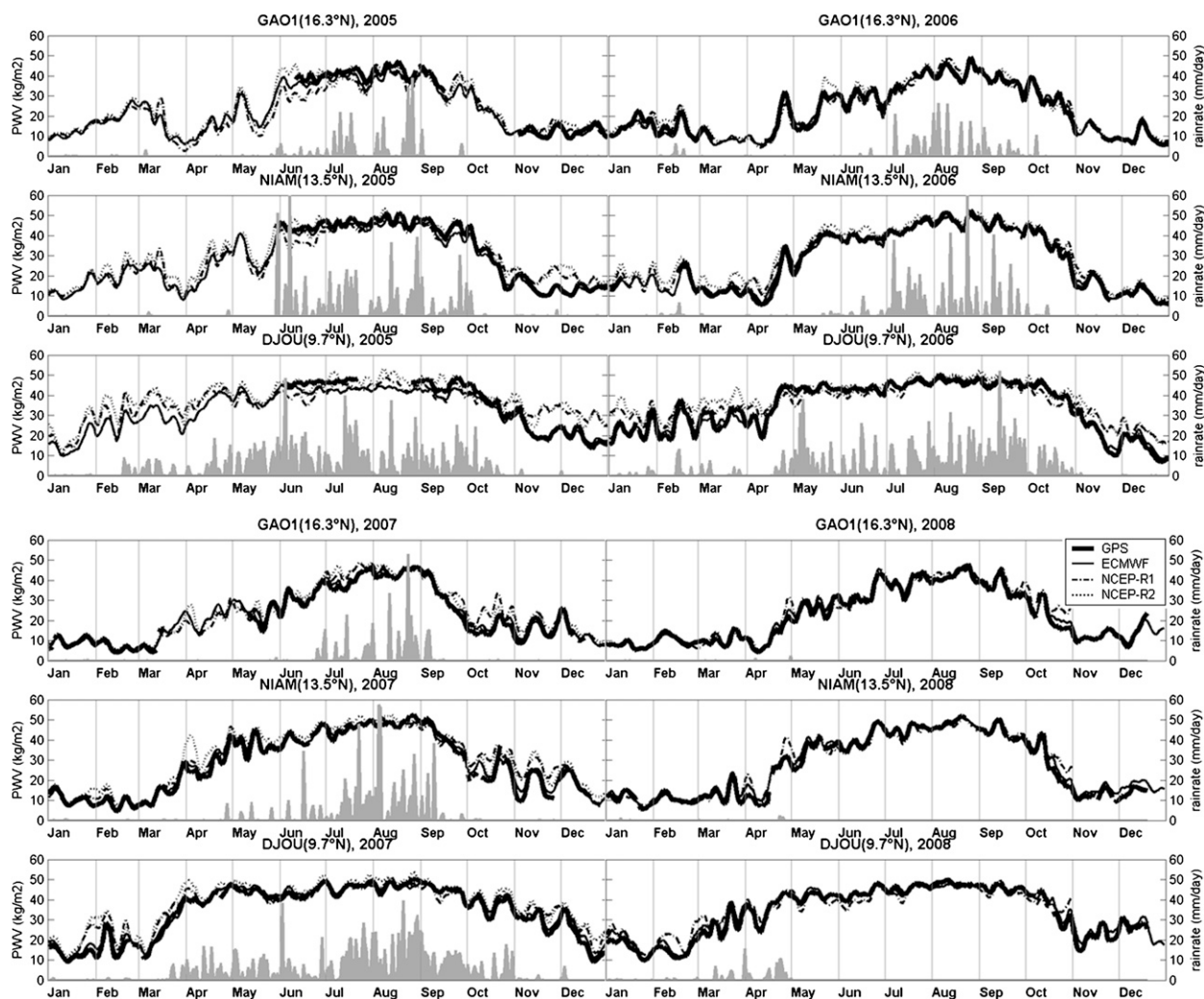


FIG. 2. Time evolution of PWV estimated from three AMMA GPS stations (GAO1, NIAM, and DJOU) and corresponding values from NWP model analyses (ECMWF, NCEP1, and NCEP2), as well as the precipitation rate, from 2005 to 2008. All data are daily averages. PWV estimates are plotted as lines, with a 5-day running mean average, and GPCP (1 day, 1°) is plotted as gray shading (vertical axis on the right). At the time of writing, NCEP2 data were only available until 31 Dec 2007 and GPCP data until 30 Apr 2008.

assimilated in both systems are difficult to check unless we have access to assimilation feedback statistics. However, the impact of enhanced radiosonde data during the AMMA EOP and SOP, especially from April 2006 until the end of 2008, will be examined in the following section.

Figure 3 shows the monthly mean and standard deviation of the differences between daily averages of model PWV and GPS PWV at the same three GPS sites. Figure 3 allows us to more precisely quantify the differences between the analyses and observations and to highlight their temporal evolution (on a monthly basis). It is seen that the monthly mean bias of the ECMWF analysis is smaller than $\pm 5 \text{ kg m}^{-2}$ at Djougou, and $\pm 2 \text{ kg m}^{-2}$ at Niamey and Gao. A reduction in magni-

tude of the bias can be distinguished in 2006, as compared to 2005, which is probably linked with the change in resolution of the forecast model and assimilation of the AMMA data. However, over the time period under consideration, it seems that the bias in the ECMWF model analysis is going from negative (dry) toward positive (wet) values. The origin of this tendency is not yet explained, but it seems to be of large-scale origin as it is observed at all three stations and also at the other GPS stations (not shown). One possible explanation might be in the changes made to the model, though this is difficult to confirm. Overall, these changes do not have a strong impact in terms of PWV compared to the large seasonal variations in the PWV bias. The absolute bias is also decreasing from south to north, which

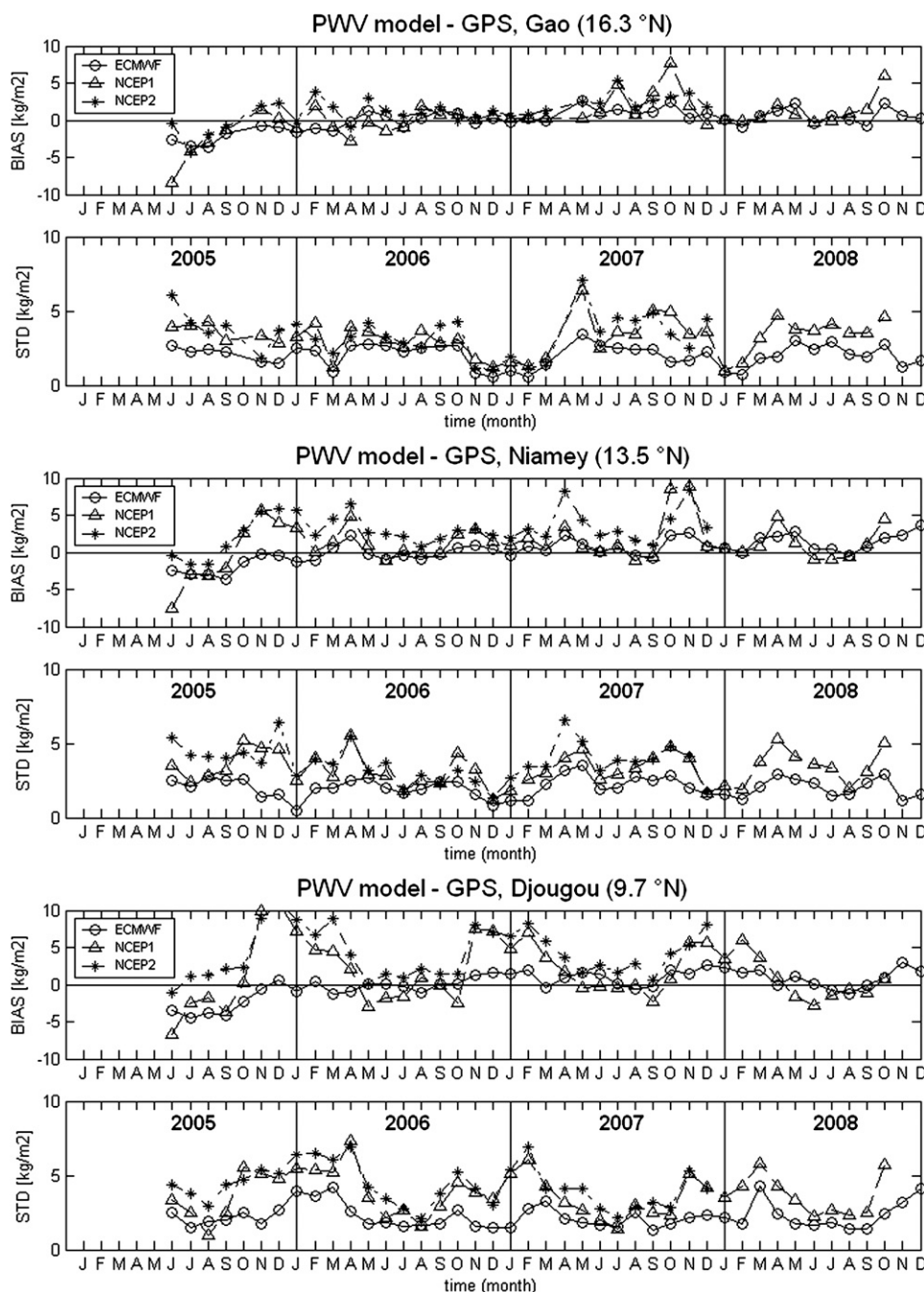


FIG. 3. Monthly mean and standard deviation of the differences between model analyses and GPS PWV estimates, at three GPS sites. The statistics are computed from daily mean data.

is consistent with the decrease in average PWV and the tendency of the model to place the ITCZ too far south (Agusti-Panareda and Beljaars 2008). The standard deviation, on the other hand, is roughly the same at all three sites, but exhibits a significant seasonal modulation, which is consistent with the seasonal variation in PWV over the region.

Both NCEP–NCAR reanalyses show a significantly larger bias and standard deviation of PWV differences as opposed to ECMWF. The bias (standard deviation) occasionally reaches 10 (7) kg m^{-2} , especially at the southern sites (e.g., Djougou seen in Fig. 3). The standard deviation shows a similar seasonal modulation as seen with ECMWF. Table 3 reports the statistics of the

TABLE 3. Differences between daily mean model PWV and GPS PWV, at the locations of eight GPS stations, over the period 1 Jan 2005–31 Dec 2007. The columns show the average PWV from GPS, mean difference (BIAS) as model PWV – GPS PWV, std dev of difference, correlation coefficient (r) between model PWV and GPS PWV, slope and offset parameters fitted as $\text{PWV}_{\text{model}} = \text{slope} \times \text{PWV}_{\text{GPS}} + \text{offset}$, and the number of data pairs (NP). The stations are ordered by increasing latitude.

GPS ID	PWV (kg m^{-2})	NP	Model	BIAS (kg m^{-2})	BIAS PWV	Std dev (kg m^{-2})	Std dev PWV	r	Slope	Offset (kg m^{-2})
TAMA	37.3	386	ECMWF	1.1	0.029	2.7	0.071	0.99	0.90	4.9
			NCEP1	2.2	0.059	5.5	0.148	0.95	0.75	11.6
			NCEP2	3.9	0.103	4.7	0.125	0.96	0.82	10.8
DJOU	34.5	898	ECMWF	−0.1	−0.002	2.8	0.083	0.98	0.90	3.5
			NCEP1	2.0	0.058	5.8	0.169	0.91	0.66	13.7
			NCEP2	4.2	0.122	5.5	0.159	0.91	0.72	13.8
OUAG	32.4	555	ECMWF	0.9	0.027	2.3	0.072	0.99	0.95	2.3
			NCEP1	1.0	0.032	3.9	0.120	0.97	0.90	4.5
			NCEP2	2.6	0.080	3.7	0.113	0.97	0.94	4.6
NIAM	29.9	881	ECMWF	−0.1	−0.003	2.6	0.087	0.99	0.93	2.0
			NCEP1	1.1	0.036	4.5	0.148	0.96	0.84	5.8
			NCEP2	2.7	0.091	4.2	0.140	0.96	0.89	6.2
DAKA	28.0	350	ECMWF	1.0	0.037	2.3	0.084	0.99	0.90	3.9
			NCEP1	−1.3	−0.045	3.9	0.138	0.96	0.81	4.0
			NCEP2	0.8	0.027	4.5	0.159	0.95	0.77	7.2
GAO1	24.7	766	ECMWF	−0.1	−0.002	2.6	0.106	0.98	0.95	1.1
			NCEP1	0.4	0.015	4.2	0.168	0.95	0.93	2.2
			NCEP2	1.3	0.051	3.9	0.158	0.96	0.93	3.1
TOMB	23.5	618	ECMWF	0.8	0.034	2.6	0.111	0.98	0.96	1.7
			NCEP1	0.2	0.008	3.9	0.167	0.96	0.94	1.5
			NCEP2	0.6	0.027	3.7	0.156	0.96	0.93	2.4
TAMP	13.9	514	ECMWF	−3.0	−0.237	2.1	0.170	0.96	0.72	0.6
			NCEP1	−2.7	−0.214	2.4	0.188	0.94	0.71	1.0
			NCEP2	−1.4	−0.107	2.3	0.179	0.93	0.82	0.9

analyses differences for all sites and all three models during 2005–07. Note that the standard deviation of the error decreases with latitude for both NCEP–NCAR reanalyses and that NCEP2 has, overall, smaller random errors. The bias, on the other hand, is quite large in NCEP2 at the southern stations. Overall, it is seen that PWV is higher in NCEP2 compared to NCEP1, and that both models show a too strong gradient in PWV over the area (this is reflected by the change in the sign of the bias between the southern and northern stations).

The performance of NWP analyses or reanalyses depends on which parameters and which time scales are being verified. We have shown previously that the PWV analysis differences (compared to GPS PWV) of both ECMWF reanalysis ERA-40 and NCEP2 are significantly reduced from 6-hourly (instantaneous) fields to 7-day averages over Africa (Bock et al. 2007). Table 4 presents a nearly similar comparison but from the AMMA GPS sites during the period 2005–07. It is seen that the ECMWF operational analysis yields better agreement with GPS than did ERA-40 (Bock et al. 2007), although one should note that the domain of the verification is not exactly the same. A similar result is observed with NCEP2, while NCEP1 has slightly larger errors. This confirms that the models still have

difficulties in handling the diurnal cycle (assessed from 6-hourly data) and synoptic-scale weather systems (assessed from daily mean data). At the time scale of 5 days, the differences are significantly reduced, as is seen in the reduction in the standard deviation: by 40% for ECMWF, 33% for NCEP2, and 22% for NCEP1. The rather high correlations seen at all time resolutions in Table 4 are explained primarily by the dominant seasonal cycle variations included in the comparison.

The impact of horizontal resolution in the model analyses is inspected from the ECMWF data extracted at 0.25° , 0.5° , 1.125° , and 2.5° . Figure 4 shows the bias, standard deviation of differences, correlation coefficient, and slope parameter compared to the GPS point observation at 0000 UTC. At all resolutions, the model data were corrected for vertical displacement and interpolated bilinearly to the location of the GPS site. Overall, the impact on the correlation coefficient and standard deviation is small (there is more variability between stations than between resolutions). The bias and slope change slightly with resolution (these parameters being correlated), which might be the result of several factors. The spatial variability in PWV and the impact of topography might contribute to differences depending on the distances of the grid points from the

TABLE 4. Differences between model analysis PWV and GPS PWV (average over all eight stations) as a function of time resolution (6 hourly, daily, and 5 daily), over the period 1 Jan 2005–31 Dec 2007. Content is similar to that in Table 3.

Time	PWV (kg m^{-2})	BIAS (kg m^{-2})	BIAS PWV	STD (kg m^{-2})	STD PWV	r	Slope	Offset (kg m^{-2})	NP
ECMWF – GPS									
6 h	28.1	0.0	0.001	3.4	0.122	0.97	0.95	1.5	19 692
24 h	28.1	0.0	0.000	2.8	0.100	0.98	0.96	1.0	4999
5 d	28.0	0.0	0.001	2.3	0.080	0.99	0.98	0.6	1021
NCEP1 – GPS									
6 h	28.1	0.7	0.023	5.4	0.191	0.94	0.88	3.9	19 692
24 h	28.1	0.6	0.023	4.8	0.172	0.95	0.90	3.5	4999
5 d	28.0	0.6	0.023	4.1	0.147	0.96	0.91	3.1	1021
NCEP2 – GPS									
6 h	28.1	2.2	0.076	5.3	0.189	0.94	0.92	4.5	19 692
24 h	28.1	2.1	0.076	4.7	0.169	0.95	0.93	4.0	4999
5 d	28.0	2.1	0.076	3.8	0.137	0.97	0.95	3.5	1021

GPS station. These differences are however smoothed by the integrative effect of interpolation from the surrounding grid points. Nevertheless, it is expected and confirmed from Fig. 4 that the agreement decreases with coarser resolution (decrease in slope and slight increase in standard deviation). The reduction in bias at most sites is actually an artifact resulting from the above-mentioned compensating effects. The increase in bias at Dakar might be due to the impact of grid points over the ocean. We must also mention that there is an overall moist bias in the analysis at 0000 UTC,

which may be linked with a bias in the radiosonde data (see next section). Overall, the choice of the resolution does not change the main conclusions, but for a detailed investigation of the biases, high resolution is recommended.

4. Impact of radiosonde biases

During AMMA, different types of sondes were used, including the Vaisala RS80-A and RS92, and the Modem M2K2. Table 5 indicates that at Tamale, Ghana, Vaisala

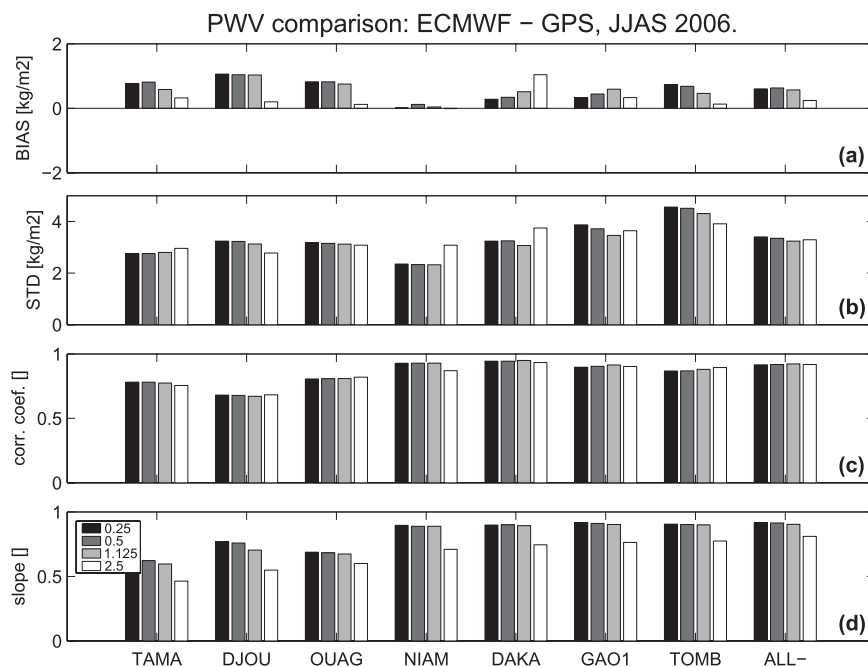


FIG. 4. Comparison of ECMWF PWV and GPS PWV: (a) mean and (b) standard deviation of the differences, (c) correlation coefficient, and (d) slope of the least squares fit. Results are presented as a function of model resolution (from 0.25° to 2.5°), at seven stations and the average over stations (last column). The statistics are computed for 0000 UTC, over the period June–September 2006.

TABLE 5. Locations of RS stations, types of sondes, and displacements w.r.t. GPS sites (GPS – RS). At some sites, different types of sondes have been used alternatively over the period of study (2006–08). The stations are ordered by increasing latitude.

RS ID	Location	Type of sonde	Lat (°N)	Lon (°E)	Alt (m)	GPS ID	Horizontal displacement (km)	Vertical displacement (m)
65418	Tamale	RS92	9.6	−0.8	168	TAMA	1	2
65330	Parakou	Modem	9.4	2.6	393	DJOU	110	43
65503	Ouagadougou	Modem	12.4	−1.5	306	OUAG	1	−1
61052	Niamey	RS80A–RS92	13.5	2.2	227	NIAM	3	−4
61641	Dakar	RS80A–RS92	14.7	−17.5	24	DAKA	6	−8
61223	Tombouctou	RS80A–RS92	16.7	−3.0	263	TOMB	1	0

RS92 sondes were used exclusively, while at Dakar, Niamey, and Timbuktu (Tombouctou), Mali, both RS80-A and RS92 sondes were used (Fig. 5 below indicates when they were used). At other sites not considered here, only Vaisala RS80-A (e.g., Bamako, Mali; Agadez, Niger; Nouadhibou and Nouakchott, Mauritania) or RS92 (e.g., Abuja, Nigeria) were used. At Pakarou, Benin, and Ouagadougou, Burkina Faso, only Modem sondes were launched. It was well known from previous experiments that RS80-A measurements have a tendency to underestimate humidity, and that this dry bias is changing with sonde age (Wang et al. 2002; Wang and Zhang 2008). For the Vaisala RS92 and Modem M2K2, very few intercomparisons were published when AMMA started; however, it became quickly evident that these more recent types of sondes also exhibit biases with a marked diurnal cycle (Bock et al. 2008a). Bock et al. (2008a) quantified the radiosonde bias by comparison with GPS PWV data during the AMMA SOP (June–September 2006). Their results show that the dry bias of the RS80-A sondes used at Dakar and Timbuktu could reach 5 kg m^{-2} at night and 8 kg m^{-2} during daytime (about 20% of the PWV at Timbuktu). These results were consistent with previous results obtained in Africa (Bock et al. 2007) and in other regions of the world (Wang and Zhang 2008). These results thus motivated the development of a bias correction scheme for the AMMA radiosonde dataset (Nuret et al. 2008) but also for the AMMA reanalysis and operational assimilation of the global radiosonde network at ECMWF (Agusti-Panareda and Beljaars 2008) and Météo-France (Faccani et al. 2009). The AMMA GPS PWV data thus appeared to be extremely useful for the detection and correction of the radiosonde humidity biases and the validation of the correction schemes.

Figure 6 shows the radiosonde biases and standard deviation of the differences in PWV compared to GPS. It is seen that Vaisala RS80-A sondes have a systematic dry bias of $\sim 6 \text{ kg m}^{-2}$ on average over 0000 and 1200 UTC with a slight variation in the bias depending on time of day. The Vaisala RS92 sondes are seen to exhibit slightly smaller biases on average but the day–

night variation can be as large as or larger than that of the RS80-A sondes. Quite surprisingly, the 0000 UTC bias is positive; that is, RS92 sondes are too moist during nighttime. This finding is of importance since the Vaisala RS92 is generally considered to be a reference during the nighttime [e.g., in the ECMWF bias correction scheme; Agusti-Panareda et al. (2009)]. The origin of this moist bias is, as of yet, not explained, but is considered to be real (e.g., it cannot be explained by a bias in the GPS PWV estimates during the nighttime) as it is also reported by Cady-Pereira et al. (2008), in a comparison with microwave radiometer measurements in the United States. Wang and Zhang (2008) show also that at nighttime the Vaisala RS92 mean bias is close to zero, but their bias frequency distribution extends toward positive (wet) biases, showing that on some occasions a wet bias can be observed. This wet bias was also diagnosed with respect to the ECMWF forecasts (observation minus background) over West Africa by Agusti-Panareda et al. (2009). During the daytime, the Vaisala RS92 sondes have a weak to moderate negative bias (too dry), as seen in Fig. 5. This dry bias is most probably linked with sensor heating during daytime (Vomel et al. 2007; Wang and Zhang 2008; Yoneyama et al. 2008). A difference can be noticed in the diurnal cycle of the Vaisala RS92 sites at Niamey and Tamale. This may be due to the different radiosonde equipment used (Digicora III at Tamale and Digicora II at Niamey; Agusti-Panareda et al. 2009). The Modem M2K2 sondes at Ouagadougou are seen to have similar deficiencies as those of the Vaisala RS92 sondes (moist bias at night and dry bias during the day), though the variation between 0000 and 1200 UTC is larger. Similar day–night differences are observed at Parakou, but with an offset (approximately +10%) toward moister values. The origin of this offset is thought to be linked with known failures in the radiosonde ground calibration system throughout most of the period at that particular site. Hence, we prefer to use the results for Ouagadougou and consider them to be representative of the Modem M2K2 sondes. After 1 January 2008 a new type of Modem sonde was launched at Ouagadougou and generally

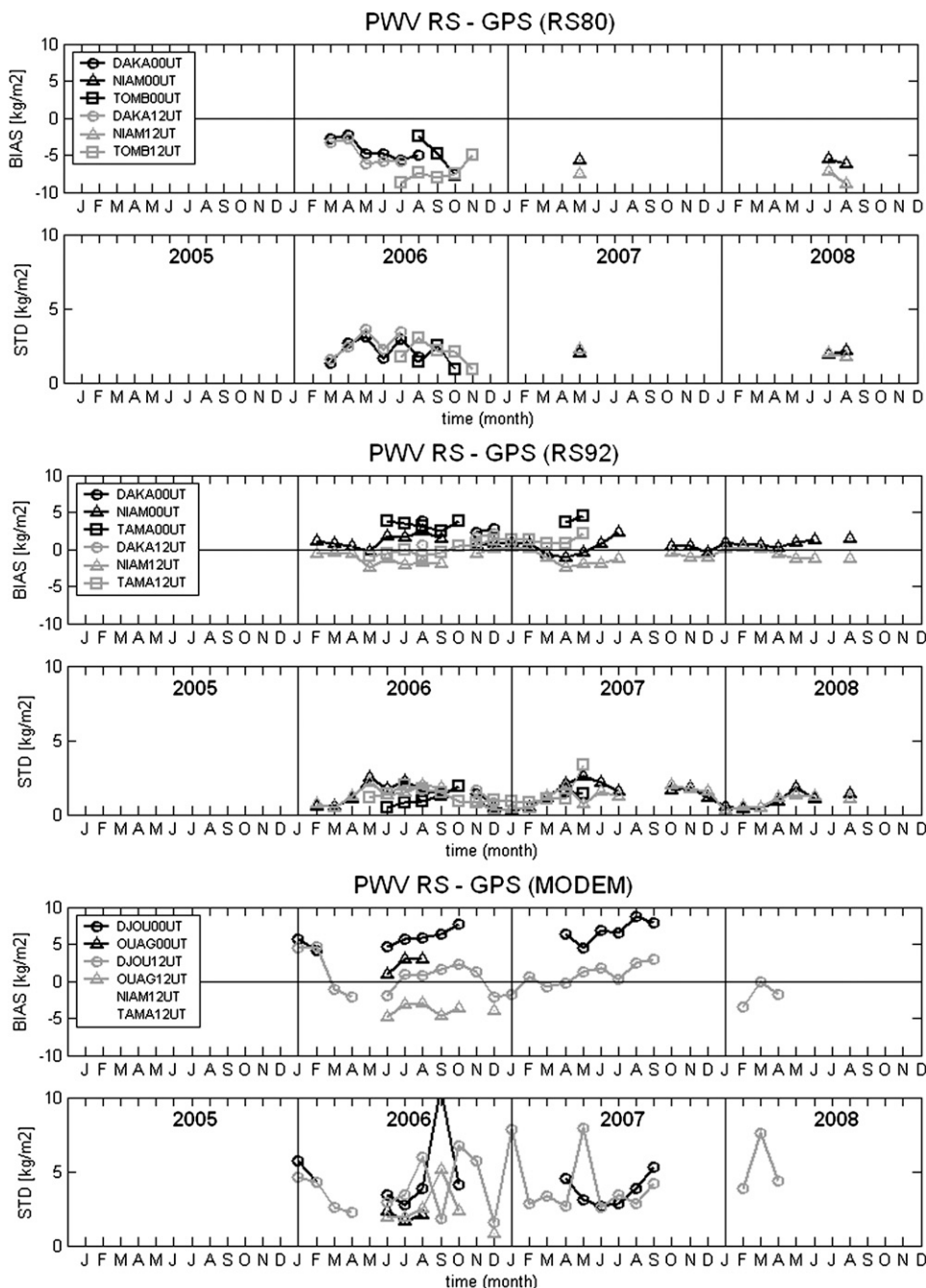


FIG. 5. Monthly mean and standard deviation of differences between daily averages of radiosonde PWV and GPS PWV as a function on sonde type (RS80-A, RS92, and MODEM) and time of day (0000 and 1200 UTC). The comparison includes only high-resolution soundings for which the sonde types were known from their serial numbers (i.e., over the period 2006–08).

in Africa (Modem M2K2-DC) with unknown humidity biases characteristics.

The standard deviation of the PWV differences (Fig. 5) is similar for the two Vaisala sondes and smaller than that of the Modem M2K2 sondes. The dispersion of the standard deviation shows a seasonal modulation for

the Vaisala sondes whereas it is quite erratic for the MODEM sondes. Table 6 presents a summary comparison for all stations and sonde types at both 0000 and 1200 UTC. It is clear from the reported diagnostics that the quality of the Vaisala RS92 sondes is superior to the older RS80-As and also superior to the Modem sondes

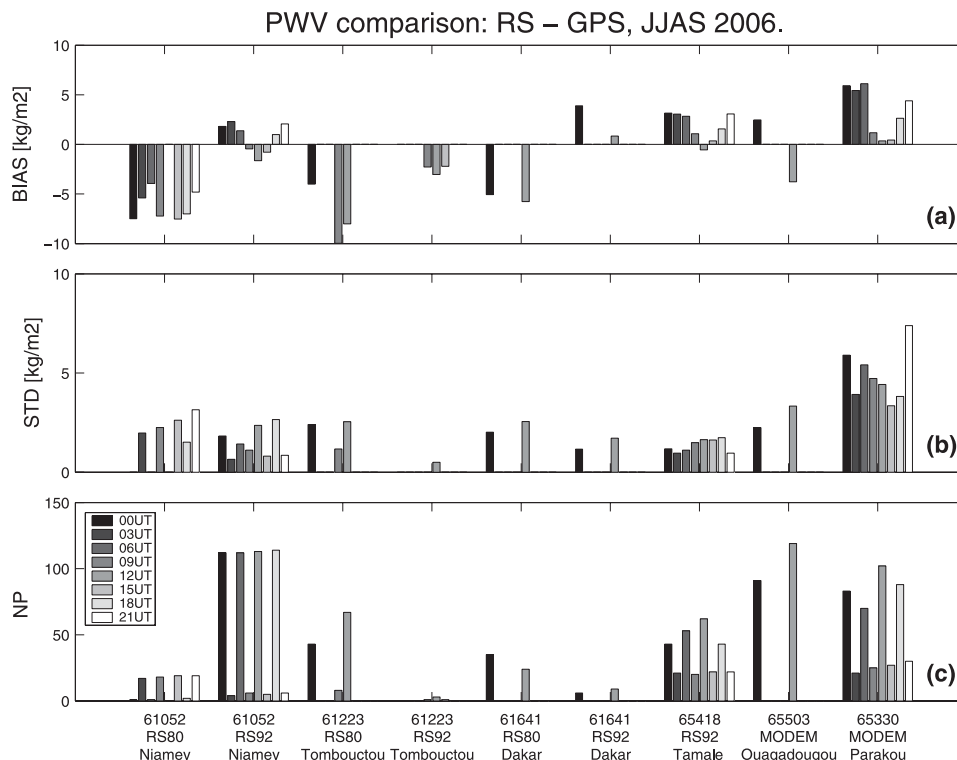


FIG. 6. (a) Mean and (b) standard deviation of differences between RS PWV and GPS PWV; (c) number of data pairs. Results are presented as a function of time of sonde launch (0000–2100 UTC) and sonde type, at six stations. Sonde identification code, sonde type, and location are indicated at the bottom of the panel. The statistics are computed over the period June–September 2006.

present in the AMMA database at the time of writing. In the future, it is expected that the correction of all the radiosonde data would yield a more homogeneous dataset.

Though large radiosonde humidity biases have been diagnosed, their impacts on NWP model analyses are difficult to define. No clear correlation arises from the comparison of the radiosonde biases displayed in Fig. 5 and the NWP model analysis biases displayed in Fig. 3. This statement holds also for the other stations not displayed in Fig. 3. In particular, one would have expected a reduction in the ECMWF model analysis bias after November 2007, when the ECMWF radiosonde bias correction scheme was used operationally. This change in the bias can actually be determined when comparing the bias in 2008 to previous years. In 2008, it seems that the model analysis bias is slightly positive (too moist) all the time, whereas, for example, in 2006, it had successively dry and wet values (Fig. 3, confirmed at other stations; not shown). However, Fig. 3 does not give insight into the diurnal variations of the bias where the radiosonde bias is particularly marked.

Figure 6 shows the radiosonde humidity bias and standard deviation of the difference between GPS

PWV as a function of time of sonde launch (0000–2100 UTC) and of sonde type. Figure 6 depicts clearly the diurnal cycle in the humidity radiosonde bias for the different sondes. Figure 7 shows similar plots but for the ECMWF model operational analysis at $0.25^\circ \times 0.25^\circ$ resolution. The data have been stratified according to sonde type and time of analysis. The monitoring of radiosonde stations at ECMWF during the SOP indicates that between 50% and 100% of the data from the stations considered here arrived via the GTS (Agusti-Panareda and Beljaars 2008). A significant amount of the radiosonde data used for the computation displayed in Fig. 6 could thus be assimilated (when not rejected). The results from Fig. 7 are thus indicative of the impact of radiosonde biases on the analysis. It is clear from a comparison of Figs. 6 and 7 that there is a high degree of correlation between the radiosonde biases and analysis biases. The sign of the bias is usually conserved, but the magnitude is significantly reduced in the analysis. This bias reduction might be due to the impact of the model's first guess (the analysis lies always between the first guess and the observations) and the quality control procedure used in the ECMWF's 4DVAR system (i.e., bad or significantly biased soundings may be rejected).

TABLE 6. Differences between RS PWV and GPS PWV as a function of sonde type, over the period 2006–08. Averages are calculated over the monthly mean statistics (i.e., weighted by the number of data pairs). The total number of data pairs is reported in NP.

GPS ID	PWV	BIAS	STD	r	Slope	NP	PWV	BIAS	STD	r	Slope	NP
	(kg m ^{−2})	(kg m ^{−2})	(kg m ^{−2})				(kg m ^{−2})	(kg m ^{−2})	(kg m ^{−2})			
0000 UTC						1200 UTC						
RS80												
DAKA	29.6	−4.0	2.6	0.98	0.88	77	26.5	−4.6	3.0	0.97	0.83	71
NIAM	42.2	−5.5	2.1	0.97	0.92	69	42.0	−7.8	2.1	0.95	0.84	72
TOMB	38.0	−4.5	2.7	0.95	1.02	48	33.8	−7.5	2.4	0.98	0.88	97
Avg	36.6	−4.7	2.4	0.97	0.94	65	34.1	−6.6	2.5	0.97	0.85	80
RS92												
DAKA	25.5	2.8	1.3	1.00	1.03	27	27.0	1.4	1.5	1.00	0.96	30
NIAM	25.1	0.8	1.6	1.00	1.03	688	25.3	−1.0	1.5	1.00	0.95	683
TAMA	47.2	3.6	1.5	0.96	0.97	95	37.0	0.4	1.6	1.00	0.96	239
Avg	32.6	2.4	1.5	0.98	1.01	270	29.8	0.3	1.5	1.00	0.96	317
Modem												
DJOU	42.4	6.4	4.8	0.87	1.01	254	34.1	0.5	5.1	0.93	1.03	526
OUAG	44.4	2.3	2.2	0.94	1.10	94	40.0	−3.9	3.0	0.97	1.02	147
Avg	43.4	4.3	3.5	0.91	1.06	174	37.0	−1.7	4.0	0.95	1.03	337

With NCEP1 and NCEP2, very similar results are found in terms of the correlation of the diurnal model bias variations with radiosonde bias variations (not shown). For NCEP1 the sign of the bias is correct but the magnitude is generally larger than for ECMWF-IFS. For NCEP2, there is roughly an offset toward a wetter bias

compared to NCEP1, which is consistent with the results reported above.

5. Conclusions and discussion

This paper assessed the performance of global NWP models (ECMWF-IFS operational analysis, and NCEP–

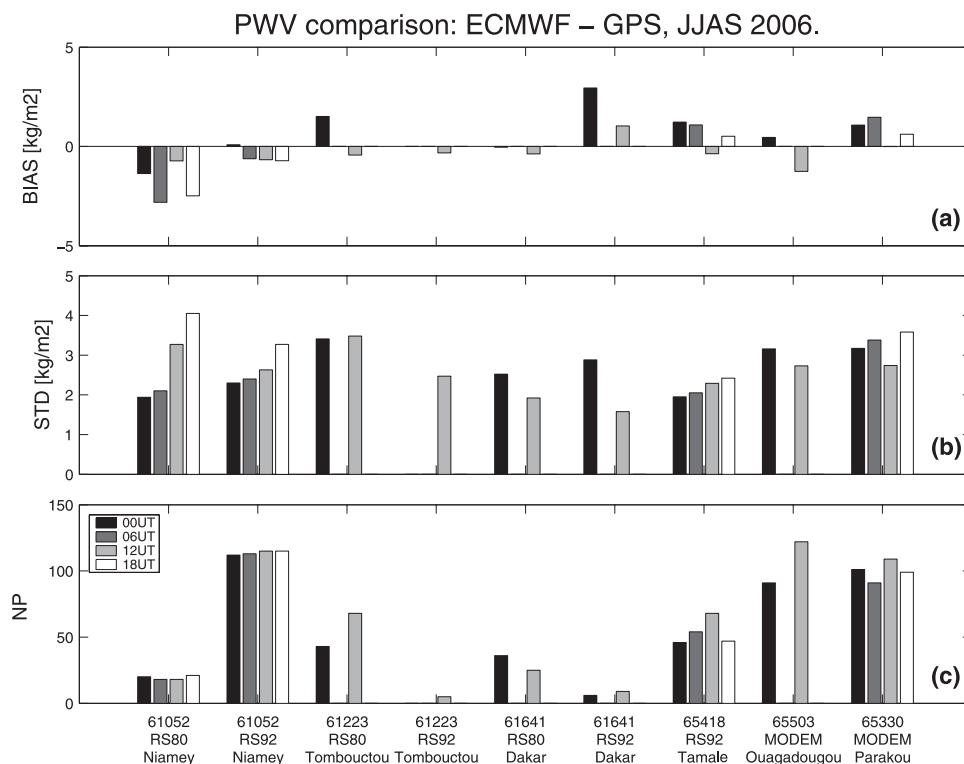


FIG. 7. Similar to Fig. 6 but for the ECMWF analysis minus GPS. The data pairs have been stratified according to sonde type and time of sonde launch in 6-h bins. Note the change in vertical scale between Figs. 7 and 6.

NCAR reanalyses I and II) over West Africa, using mainly PWV retrievals from a ground-based GPS network operated during AMMA. A comparison of surface parameters (2-m humidity and temperature from the GPS weather stations) showed that all three NWP model datasets are in close agreement with the observations, though the NCEP–NCAR reanalyses have larger errors (mean and standard deviation).

The model errors diagnosed w.r.t. to GPS PWV have been analyzed at different time scales, from 6-hourly to monthly. All three models show reasonable agreement with GPS PWV at monthly time scales, though the NCEP–NCAR reanalyses show significant overestimations in PWV at southern sites. The differences have a tendency to increase as one goes from 5-daily mean PWV to 6-hourly (instantaneous) PWV. This reflects the increased difficulty of the model to handle humidity variations associated with synoptic-scale disturbances and the diurnal cycle. The simulation of such features is highly parameterized in global NWP models. The higher horizontal resolution of the native ECMWF-IFS model and the more recent versions of convection schemes employed might explain the better agreement with the GPS PWV observations over this range of time scales (the RMSE being reduced by a factor of ~ 2 compared to the NCEP–NCAR reanalyses). However, a clear correlation between ECMWF-IFS model changes and the PWV error could not be established over the period of study (2005–08). On the other hand, the impact of radiosonde humidity biases could be evidenced at the level of the diurnal cycle. The results point to dry biases in the ECMWF analysis when Vaisala RS80-A soundings were assimilated (at Niamey), and wet biases when RS92 or MODEM soundings were assimilated (at Dakar, Tamale, Ouagadougou, and Parakou).

A correction scheme for the radiosonde humidity bias was introduced into the ECMWF operational assimilation system on 6 November 2007 (Agusti-Panareda and Beljaars 2008). This scheme accounts for sonde type, solar elevation, and altitude, and uses the model first guess as an intermediate dataset for computing biases. The bias correction coefficients are based on the difference between the bias of the sonde type to be corrected and the bias of the RS92 sonde during the nighttime taken as a reference (the bias is computed w.r.t. the model first guess). A refined version has been developed by Agusti-Panareda et al. (2009) for the AMMA reanalysis, which depends also on the observed RH. A comparison with GPS PWV shows that this scheme is effective at reducing the dry bias of the RS80-A soundings by between 1 and 4 kg m⁻² and the daytime dry bias of the RS92 and Modem soundings by ~ 1 kg m⁻². As a consequence, the systematic error in the lo-

cation of the ITCZ is slightly reduced and precipitation forecasts are improved in the short range. The refined version of the ECMWF scheme has been tested at Météo-France in the ARPEGE system in addition to modifications allowing the assimilation of new Advanced Microwave Sounding Unit-B (AMSU-B) channels (Karbou et al. 2008, manuscript submitted to *Wea. Forecasting*; Faccani et al. 2009). The combination of both modifications provides clearly improved analyses and forecasts over the AMMA region (reduced surface humidity bias, improved precipitation scores, higher PWV contents in agreement with GPS observations, and downstream propagation of reduced geopotential height error). In parallel with the development of an operational correction scheme, a more physically based scheme is being developed at the Centre National De Recherches Météorologiques (CNRM), Météo-France (Nuret et al. 2008). The new method also uses nighttime results from the Vaisala RS92 as the reference sonde for correcting the RS80-A data. Hence, it appears that the absolute bias of the nighttime Vaisala RS92 is now an issue, and needs to be perfectly known. According to Fig. 6, it is seen that this sonde exhibits a nighttime wet bias of 2–3 kg m⁻², which is consistent with the results from Cady-Pereira et al. (2008).

The comparison of RS92 measurements to a reference sonde such as a chilled mirror hygrometer (Fujiwara et al. 2003) should help in evaluating this nighttime bias, as well as the daytime dry bias in the RS92 for which the radiation effects seem to be presently undercorrected by the operational radiosonde station software (see Fig. 6). An experiment was conducted in Niamey during summer 2008 to document the Vaisala RS92 and Modem M2K2 biases as compared to the Swiss Snow-White chilled mirror hygrometer. This dataset should improve the present correction scheme and allow for a fine correction of all AMMA radiosondes (M. Nuret 2008, personal communication). Such a correction is especially required for computing water budgets from observations (e.g., Zangvil et al. 2001).

The recent improvements of NWP models (e.g., radiosonde bias correction and assimilation of AMSU-B channels sensitive to humidity in the lower troposphere) should lead to improved forecast skill for precipitation over West Africa. It should also allow the computation of more accurate water budgets, especially at regional scales, for which NWP models are especially useful at estimating moisture flux divergence and tendency terms (Higgins et al. 1996; Trenberth and Guillemot 1998; Roads et al. 2002; Bock et al. 2008b). Understanding the water cycle of the WAM is a fundamental objective of AMMA, which will remain a focus of sustained work in the future.

Acknowledgments. The authors thank M.N. Bouin, CNRM/Météo-France, for processing the GPS data and E. Doerflinger, CNRS, among others for helping establish the GPS network in Africa [see Bock et al. (2008a) for a full list of participants]. The authors acknowledge J.-P. Lafore and F. Guichard, CNRM/Météo-France, as well as A. Agusti-Panareda, ECMWF, for numerous discussions about radiosonde biases and their impact on NWP model analyses. The authors also acknowledge L. Fleury, AMMA Project, for retrieving the radiosonde data and serial numbers, and S. Bouffies-Cloche, IPSL/CNRS, for retrieving the NWP model analyses.

Based on a French initiative, AMMA was built by an international scientific group and is currently funded by a large number of agencies, especially from France, the United Kingdom, the United States, and Africa. The project has been the beneficiary of a major financial contribution from the European Community's Sixth Framework Research Programme. Detailed information on scientific coordination and funding is available on the AMMA International Web site (<http://www.amma-international.org>).

REFERENCES

- Agusti-Panareda, A., and A. Beljaars, 2008: ECMWF's contribution to AMMA. *ECMWF Newsletter*, No. 115, ECMWF, Reading, United Kingdom, 19–27.
- , and Coauthors, 2009: Radiosonde humidity bias correction over the West African region for the special AMMA reanalysis at ECMWF. *Quart. J. Roy. Meteor. Soc.*, **135**, 595–617.
- Andersson, E., and Coauthors, 2005: Assimilation and modeling of the atmospheric hydrological cycle in the ECMWF forecasting system. *Bull. Amer. Meteor. Soc.*, **86**, 387–402.
- , and Coauthors, 2007: Analysis and forecast impact of the main humidity observing systems. *Quart. J. Roy. Meteor. Soc.*, **133**, 1473–1485.
- Bechtold, P., M. Koehler, T. Jung, F. Doblas-Reyes, M. Leutbecher, M. J. Rodwell, F. Vivart, and G. Balsamo, 2008: Advances in simulating atmospheric variability with the ECMWF model: From synoptic to decadal time scales. *Quart. J. Roy. Meteor. Soc.*, **134**, 1337–1351.
- Bevis, M., S. Businger, S. Chiswell, T. A. Herning, R. A. Anthes, C. Rocken, and R. H. Ware, 1994: GPS Meteorology: Mapping zenith wet delay onto precipitable water. *J. Appl. Meteor.*, **33**, 379–386.
- Bock, O., M.-N. Bouin, A. Walpersdorf, J.-P. Lafore, S. Janicot, F. Guichard, and A. Agusti-Panareda, 2007: Comparison of ground-based GPS precipitable water vapour to independent observations and numerical weather prediction model reanalyses over Africa. *Quart. J. Roy. Meteor. Soc.*, **133**, 2011–2027.
- , and Coauthors, 2008a: The West African monsoon observed with ground-based GPS receivers during AMMA. *J. Geophys. Res.*, **113**, D21105, doi:10.1029/2008JD010327.
- , R. Meynadier, F. Guichard, P. Roucou, A. Boone, J. L. Redelsperger, and S. Janicot, 2008b: Assessment of water budgets computed from NWP models and observational datasets during AMMA-EOP. Preprints, *28th Conf. on Hurricanes and Tropical Meteorology*, Orlando, FL, Amer. Meteor. Soc., 3C.3. [Available online at <http://ams.confex.com/ams/pdfpapers/138101.pdf>.]
- Cady-Pereira, K. E., M. W. Shephard, D. D. Turner, E. J. Mlawer, S. A. Clough, and T. J. Wagner, 2008: Improved daytime column-integrated precipitable water vapor from Vaisala radiosonde humidity sensors. *J. Atmos. Oceanic Technol.*, **25**, 873–883.
- Deblonde, G., S. Macpherson, Y. Mireault, and P. Héroux, 2005: Evaluation of GPS precipitable water over Canada and the IGS network. *J. Appl. Meteor.*, **44**, 153–166.
- Faccani, C., and Coauthors, 2009: The impacts of AMMA radiosonde data on the French global assimilation and forecast system. *Wea. Forecasting*, in press.
- Fujiwara, M., M. Shiotani, F. Hasebe, H. Vömel, S. J. Oltmans, P. W. Ruppert, T. Horinouchi, and T. Tsuda, 2003: Performance of the Meteorolabor “Snow White” chilled-mirror hygrometer in the tropical troposphere: Comparisons with the Vaisala RS80 A/H-humicap sensors. *J. Atmos. Oceanic Technol.*, **20**, 1534–1542.
- Haase, J. S., M. Ge, H. Vedel, and E. Calais, 2003: Accuracy and variability of GPS tropospheric delay measurements of water vapor in the Western Mediterranean. *J. Appl. Meteor.*, **42**, 1547–1568.
- Hagemann, S., L. Bengtsson, and G. Gendt, 2003: On the determination of atmospheric water vapor from GPS measurements. *J. Geophys. Res.*, **108**, 4678, doi:10.1029/2002JD003235.
- Higgins, R. W., K. C. Mo, and S. D. Schubert, 1996: The moisture budget of the central United States in spring as evaluated in the NCEP-NCAR and the NASA/DAO reanalyses. *Mon. Wea. Rev.*, **124**, 939–963.
- Huffman, G., and Coauthors, 1997: The Global Precipitation Climatology Project (GPCP) combined precipitation dataset. *Bull. Amer. Meteor. Soc.*, **78**, 5–20.
- Karbou, F., F. Rabier, J.-P. Lafore, J.-L. Redelsperger, and O. Bock, 2008: Global 4DVAR assimilation and forecast experiments using land surface emissivities from AMSU-A and AMSU-B. Part II: Impact of adding surface channels on the African monsoon during AMMA. *Wea. Forecasting*, submitted.
- Kalnay, E., and Coauthors, 1996: The NCEP/NCAR 40-Year Reanalysis Project. *Bull. Amer. Meteor. Soc.*, **77**, 437–471.
- Kanamitsu, M., W. Ebisuzaki, J. Woollen, S.-K. Yang, J. J. Hnilo, M. Fiorino, and G. L. Potter, 2002: NCEP–DOE AMIP-II Reanalysis (R-2). *Bull. Amer. Meteor. Soc.*, **83**, 1631–1643.
- Klein Baltink, H., H. van der Marel, and A. G. A. van der Hoeven, 2002: Integrated atmospheric water vapour estimates from a regional GPS network. *J. Geophys. Res.*, **107**, 4025, doi:10.1029/2000JD000094.
- Macpherson, S. R., G. Deblonde, J. M. Aparicio, and B. Casati, 2008: Impact of ground-based GPS observations on the Canadian Regional Analysis and Forecast System. *Mon. Wea. Rev.*, **136**, 2727–2746.
- Nuret, M., J.-P. Lafore, N. Asencio, H. Bénichou, O. Bock, F. Favot, T. Montmerle, and Y. Seity, 2007: Evaluation of METEO-FRANCE NWP models during AMMA 2006-SOP. *Aladin Newsl.*, **32**, 93–107.
- , —, O. Bock, F. Guichard, A. Agusti-Panareda, J.-B. Ngamini, and J.-L. Redelsperger, 2008: Correction of humidity bias for Vaisala RS80 sondes during the AMMA 2006 observing period. *J. Atmos. Oceanic Technol.*, **25**, 2152–2158.

- Parker, D. J., and Coauthors, 2008: The AMMA Radiosonde Programme and its implications for the future of atmospheric monitoring over Africa. *Bull. Amer. Meteor. Soc.*, **89**, 1015–1027.
- Redelsperger, J.-L., C. Thorncroft, A. Diedhiou, T. Lebel, D. J. Parker, and J. Polcher, 2006: African Monsoon Multi-disciplinary Analysis (AMMA): An international research project and field campaign. *Bull. Amer. Meteor. Soc.*, **87**, 1739–1746.
- Roads, J., M. Kanamitsu, and R. Stewart, 2002: CSE water and energy budgets in the NCEP–DOE reanalysis II. *J. Hydro-meteor.*, **3**, 227–248.
- Sultan, B., and S. Janicot, 2003: West African monsoon dynamics. Part II: The “preonset” and the “onset” of the summer monsoon. *J. Climate*, **16**, 3407–3427.
- Tompkins, A. M., A. Diongue-Niang, D. J. Parker, and C. D. Thorncroft, 2005: The African easterly jet in the ECMWF Integrated Forecast System: 4D-Var analysis. *Quart. J. Roy. Meteor. Soc.*, **131**, 2861–2885.
- Trenberth, K. E., and C. J. Guillemot, 1998: Evaluation of the atmospheric moisture and hydrologic cycle in the NCEP/NCAR reanalyses. *Climate Dyn.*, **14**, 213–231.
- Vomel, H., and Coauthors, 2007: Radiation dry bias of the Vaisala RS92 humidity sensor. *J. Atmos. Oceanic Technol.*, **24**, 953–963.
- Wang, J., and L. Zhang, 2008: Systematic errors in global radiosonde precipitable water data from comparisons with ground-based GPS measurements. *J. Climate*, **21**, 2218–2238.
- , J. H. Cole, D. J. Carlson, E. R. Miller, K. Beierle, A. Paukkunen, and T. K. Laine, 2002: Corrections of humidity measurement errors from the Vaisala RS80 radiosonde—Application to TOGA COARE data. *J. Atmos. Oceanic Technol.*, **19**, 981–1002.
- Yang, G. Y., and J. Slingo, 2001: The diurnal cycle in the tropics. *Mon. Wea. Rev.*, **129**, 784–801.
- Yoneyama, K., M. Fujita, N. Sato, M. Fujiwara, Y. Inai, and F. Hasebe, 2008: Correction for radiation dry bias found in RS92 radiosonde data during the MISMO field experiment. *Sci. Online Lett. Atmos.*, **4**, 13–16.
- Zangvil, A., D. H. Portis, and P. J. Lamb, 2001: Investigation of the large-scale atmospheric moisture field over the midwestern United States in relation to summer precipitation. Part I: Relationships between moisture budget components on different timescales. *J. Climate*, **14**, 582–597.